

## Efficiency of a solar cell with intermediate energy levels: An example study on hydrogen implanted Si solar cells

Masaya Ichimura, Hiromu Sakakibara, Koji Wada, and Masashi Kato

Citation: [Journal of Applied Physics](#) **114**, 114505 (2013); doi: 10.1063/1.4821286

View online: <http://dx.doi.org/10.1063/1.4821286>

View Table of Contents: <http://scitation.aip.org/content/aip/journal/jap/114/11?ver=pdfcov>

Published by the [AIP Publishing](#)

---

### Articles you may be interested in

[Deep-level transient spectroscopy of Al/a-Si:H/c-Si structures for heterojunction solar cell applications](#)

J. Appl. Phys. **116**, 234501 (2014); 10.1063/1.4904082

[Defect density and recombination lifetime in microcrystalline silicon absorbers of highly efficient thin-film solar cells determined by numerical device simulations](#)

J. Appl. Phys. **94**, 1035 (2003); 10.1063/1.1577813

[Analysis of recombination centers in epitaxial silicon thin-film solar cells by temperature-dependent quantum efficiency measurements](#)

Appl. Phys. Lett. **82**, 2637 (2003); 10.1063/1.1566481

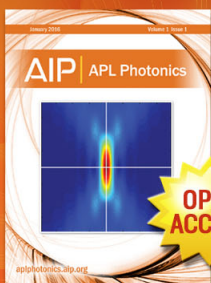
[Majority- and minority-carrier deep level traps in proton-irradiated n + /p -InGaP space solar cells](#)

Appl. Phys. Lett. **81**, 64 (2002); 10.1063/1.1491005

[Deep level analysis of radiation-induced defects in Si crystals and solar cells](#)

J. Appl. Phys. **86**, 217 (1999); 10.1063/1.370698

---



Launching in 2016!  
The future of applied photonics research is here

AIP | APL  
Photonics

## Efficiency of a solar cell with intermediate energy levels: An example study on hydrogen implanted Si solar cells

Masaya Ichimura, Hiromu Sakakibara, Koji Wada, and Masashi Kato

*Department of Engineering Physics, Electronics, and Mechanics, Nagoya Institute of Technology, Gokiso, Showa, Nagoya 466-8555, Japan*

(Received 18 June 2013; accepted 31 August 2013; published online 18 September 2013)

For any pn junction solar cell, there is a theoretical limit to its conversion efficiency, which is determined by its band gap. This efficiency may exceed the limit by introducing an intermediate level (IL) that can facilitate the sub-band-gap optical absorption, but the IL can simultaneously enhance the carrier recombination rate. To understand the net effects of the IL, it is necessary to estimate the rates of both the optical absorption and carrier capture via the IL. In this study, trap parameters and the optical absorption coefficient are evaluated for defect levels in hydrogen implanted silicon wafers using deep level transient spectroscopy, the optical-capacitance transient spectroscopy, and carrier lifetime measurements. Using the obtained trap parameters, the characteristics of hydrogen implanted silicon solar cells are simulated. The simulation results indicate that it is not possible to realize improvements in efficiency by performing hydrogen implantation. © 2013 AIP Publishing LLC. [<http://dx.doi.org/10.1063/1.4821286>]

### I. INTRODUCTION

The energy conversion efficiency of a conventional pn junction solar cell is limited by the band gap ( $E_g$ ) of the material used because photons with energy  $h\nu < E_g$  cannot be absorbed. As  $E_g$  decreases, a larger number of photons can be absorbed and the output current increases, but the output voltage decreases because the excited carriers lose the energy of  $h\nu - E_g$  in the relaxation process within the material. The limiting efficiency was first calculated by Shockley and Queisser based on the principle of detailed balance, where the recombination of carriers is considered to be radiative.<sup>1</sup> They also recognized that in an actual cell, recombination is in fact mostly nonradiative, and introduced a factor  $f_c$  that represents a fraction of the recombination current which is radiative. The limiting efficiency of a Si solar cell is about 30% if  $f_c = 1$ , and about 20% if  $f_c = 10^{-3}$ .

To overcome this limit, a solar cell with an intermediate band (IB) or level was proposed.<sup>2</sup> If there is an intermediate energy level in the band gap, an electron can be excited from the valence band to conduction band by a two-step excitation via the intermediate level (IL). The intermediate energy level can be introduced as a native defect or impurity level, or as an energy level of a quantum structure (well or dot). When an impurity is adopted to introduce the IL, the two-step carrier generation is called an impurity photovoltaic effect. If the volume density of the intermediate states is sufficiently large, an IB is formed and carriers can move in it. Otherwise, the introduced state is discreet and should be called an intermediate level or state. (In previous studies, the term “intermediate band” has been used even when carrier transport in the intermediate band is neglected.)

The IL can enhance photo absorption and thus quantum efficiency in the sub-band-gap region, while simultaneously acting as a recombination center of carriers. The recombination center will decrease concentrations of photo-generated carriers and reduce the photocurrent. In addition, it will

enhance the recombination of majority carriers. Thus, the dark forward current will increase and the output voltage can therefore be decreased. If the effects of recombination enhancement are more dominant than those of sub-band-gap absorption, the efficiency should decrease rather than increase when an intermediate level is introduced. Shockley and Queisser therefore criticized the concept of IL cells immediately after it was proposed.<sup>1</sup> Subsequently, many theoretical studies have been done on IL solar cells, and most of them predict an increase in the efficiency upon introduction of the IL.<sup>3–10</sup> However, it is often assumed that the recombination via the IL is solely radiative, i.e., the same transition probability can be applied for both the photo-excitation and recombination processes. This calculation is useful to estimate the ideal theoretical limit, but cannot be considered realistic because the nonradiative recombination is always non-negligible, and is often much more dominant than the radiative recombination. It was claimed that the nonradiative recombination would be suppressed if the intermediate band is formed, i.e., the wavefunction of the IL is delocalized,<sup>11,12</sup> but this claim was subsequently challenged based on the fact that the wavefunction will be localized during the recombination process.<sup>13</sup> Thus, it is not certain that there is an actual material system where the nonradiative recombination rate is sufficiently small for an efficiency enhancement. In fact, many prior theoretical studies are based on a generalized quantum-mechanical and thermodynamical model and are not for a specific material system. Thus, the thermal capture rates were, if not neglected, just assumed and were not based on experimental data.<sup>10</sup>

The only exception would be In in Si: several research groups reported the results of efficiency calculations that were based on experimentally determined defect parameters.<sup>14–17</sup> For In in Si, the energy level is known, and some limited information on the optical absorption is available. However, the capture cross section does not seem to be accurately known. Two groups predicted an increase in

efficiency due to the introduction of In,<sup>13,14</sup> while another reported that the improvement is negligible.<sup>16</sup> This contradiction is due to the fact that the two former groups used a very small value for the capture cross section for holes (of the order of  $10^{-22}$  cm<sup>2</sup>), while the latter group used a more common value ( $>10^{-17}$  cm<sup>2</sup>).<sup>17</sup>

Although there are many theoretical predictions of efficiency improvement, there are few such reports for the actual solar cell performance by introducing an IL. Li *et al.* introduced defect levels in a Si solar cell by hydrogen implantation and observed an efficiency of 35%.<sup>18</sup> However, their results were not reproduced. Then, another group found that the efficiency was decreased rather than increased by ion implantation.<sup>19</sup> For compound semiconductor solar cells, IB solar cells based on quantum structures have been proposed and fabricated,<sup>20–26</sup> but their performance is not better than that of the best GaAs solar cell.

Even without any theoretical calculation, one can easily see that the efficiency will increase if the IL has a very small capture cross section and a very large optical cross section. On the contrary, if the capture cross section is much larger, the efficiency should decrease. Thus, to assess the net effects of IL for actual material systems, it is necessary to evaluate both the photo absorption rate (optical cross section) and the carrier capture rate (capture cross section) by performing independent experiments. In this study, we first investigate properties of defects in Si introduced by hydrogen implantation. As detailed in Sec. II, the energy level, the thermal capture cross section, and optical (photoionization) cross section are evaluated by deep level transient spectroscopy (DLTS), optical-capacitance-transient spectroscopy (O-CTS), and carrier lifetime measurements. Then, based on the obtained defect properties, we simulate the performance of the solar cell with the defect levels, and discuss whether or not the efficiency can be improved by hydrogen implantation. It should be stated here that the hydrogen-implanted Si cell is investigated just as a first example. We believe that such experimentation must be done for any of the proposed IL solar cells.

## II. CHARACTERIZATION OF DEFECTS INTRODUCED BY HYDROGEN IMPLANTATION

### A. Experimental procedure

N-type (100) Si wafers (2–5  $\Omega$  cm) were hydrogen-implanted with doses of  $1 \times 10^{12}$ ,  $3 \times 10^{13}$ , and  $3 \times 10^{14}$  cm<sup>-2</sup>. A Van de Graaff accelerator was used, and the ions were decelerated by an Al foil so that the resulting implantation depth was about 1  $\mu$ m for samples used for DLTS and O-CTS measurements, and 10  $\mu$ m for samples used for the lifetime measurement. For DLTS and O-CTS, AuSb was evaporated on the back side as an ohmic contact, and the samples were annealed at 320  $^{\circ}$ C for 3 min. Then, Au Schottky contacts were formed on the front (implanted) surface. The Au contact size is 3.14 mm<sup>2</sup>.

The defect energy levels and the capture cross sections for the majority carriers (electrons) were obtained by DLTS. To estimate the capture cross section for holes, the carrier lifetime was measured by the microwave photoconductivity

decay ( $\mu$ -PCD) measurement with a 10 GHz microwave probe and the excitation light of a 770 nm laser diode. We evaluated the  $1/e$  lifetime, which is defined as the time interval of the decay from the peak to  $1/e$ . The penetration depth of the excitation light is about 6.5  $\mu$ m.

The optical cross sections of the defects were evaluated by O-CTS. In the O-CTS measurements, we detected the capacitance-transient signal of a diode caused by the optical excitation of carriers from deep levels, and the signal was converted to an O-CTS spectrum by the rate window scan method.<sup>27,28</sup> For the excitation light, a 300 W Xe lamp was employed. The light was passed through a monochromator and focused onto the Schottky contact region. The Au contacts for the O-CTS measurement were thin enough (about 10 nm) to be transparent for the excitation light. At temperatures at which the thermal excitation of the carriers from the deep levels is negligible, the time constant of the transient signal is given by

$$\tau = 1/\Phi\sigma_o, \quad (1)$$

where  $\Phi$  is the photon flux and  $\sigma_o$  is the optical cross section. The spectral intensity of the light source was first measured by a power meter and was then corrected for transmission of the chamber window and the Au electrode.

### B. Experimental results

Figure 1 shows the DLTS spectra (with a time constant of 7.6 ms) before and after the  $3 \times 10^{14}$  cm<sup>-2</sup> hydrogen implantation. Three peaks (peak 1, peak 2, and peak 3) were observed for the implanted sample, while no peak was observed for the unimplanted sample, as shown in Fig. 1. Thus, the peaks are due to implantation-induced defects. The same peaks were observed for the lower-dose samples, and the defect densities obtained from the DLTS peak height were plotted against the implantation dose in Fig. 2. It should be noted that the injection-emission biases were adjusted so that the defect density at a depth of about 1  $\mu$ m was obtained from the DLTS measurement. The densities increased with the dose, and the peak 1 defect had the largest density at a high dose ( $3 \times 10^{14}$  cm<sup>-2</sup>). The energy levels (activation energy) obtained from the Arrhenius plot of the emission time constant are also given in Fig. 1. According to the

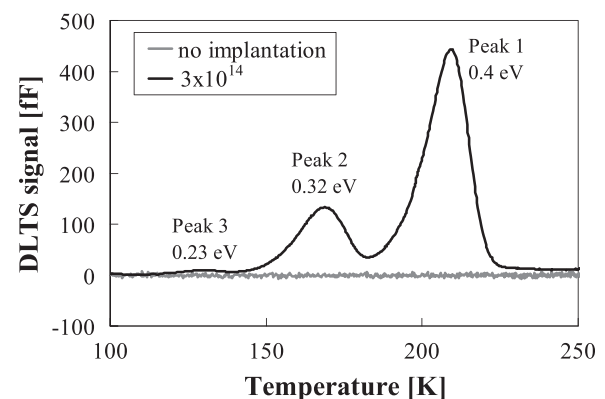


FIG. 1. DLTS spectra for the n-type Si wafers before and after  $3 \times 10^{14}$  cm<sup>-2</sup> hydrogen implantation.

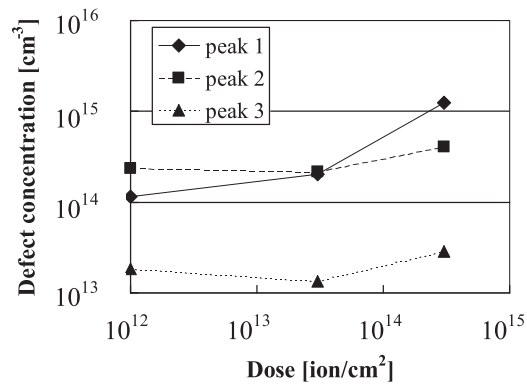


FIG. 2. Defect densities obtained from the DLTS peak height plotted against the hydrogen implantation dose.

previous studies of hydrogen-implanted Si, peak 1 could be attributed to the divacancy  $(V-V)^{0/-}$  or the phosphorus-vacancy pair  $(P-V)^{0/-}$ , peak 2 to a hydrogen-related defect, and peak 3 to the doubly negative charge state of the divacancy  $(V-V)^{-/-}$ .<sup>29,30</sup>

Table I shows the  $1/e$  lifetime for the unimplanted and implanted samples. The lifetime decreased by about one order of magnitude as a result of the  $1 \times 10^{12} \text{ cm}^{-2}$  implantation, and the implantation-induced defects therefore act as an efficient recombination center. However, the dependence on the dose is weak for the higher doses.

As noted above, the defect density is largest for peak 1 at the higher doses, and thus the peak 1 defect will be most influential on electronic and optical properties. Therefore, the optical cross section of peak 1 was evaluated by the O-CTS technique. Figure 3 shows the O-CTS spectra for the  $3 \times 10^{14} \text{ cm}^{-2}$  implanted sample at 190 K in the dark and under illumination with three different photon energies. In the dark, peaks appear at time constants of 0.025 s and 10 s. The former peak corresponds to peak 2 in Fig. 1 and the latter to peak 1. Under illumination conditions, peak 1 shifted to shorter time constants. This is because of optical excitation from the defect level to the conduction band. Since the thermal excitation is not negligible at this temperature, the emission time constant of the optical excitation is obtained by the equation

$$1/\tau = 1/\tau_o + 1/\tau_{th}, \quad (2)$$

where  $\tau$  is the observed emission time constant,  $\tau_o$  is the optical excitation time constant, and  $\tau_{th}$  is the thermal excitation time constant. The optical cross section  $\sigma_o$  was calculated from  $\tau_o$  using Eq. (1), and was plotted in Fig. 4 as a function of the photon energy. The obtained  $\sigma_o$  values are

TABLE I. Carrier lifetime of the n-type Si wafers before and after hydrogen implantation with various doses.

Dose [ $\text{cm}^{-2}$ ]	Lifetime ( $\mu\text{s}$ )
No	3.1
$1 \times 10^{12}$	0.23
$3 \times 10^{13}$	0.22
$3 \times 10^{14}$	0.52

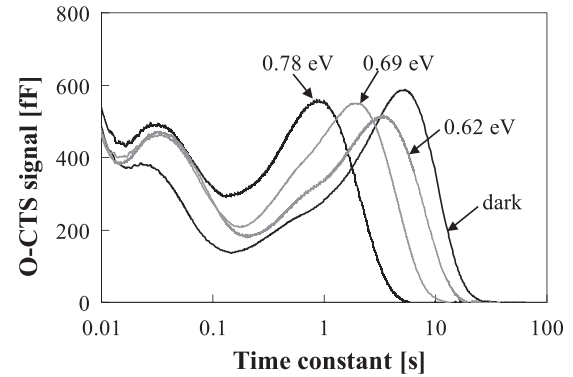


FIG. 3. O-CTS spectra at 190 K for the  $3 \times 10^{14} \text{ cm}^{-2}$  implanted sample.

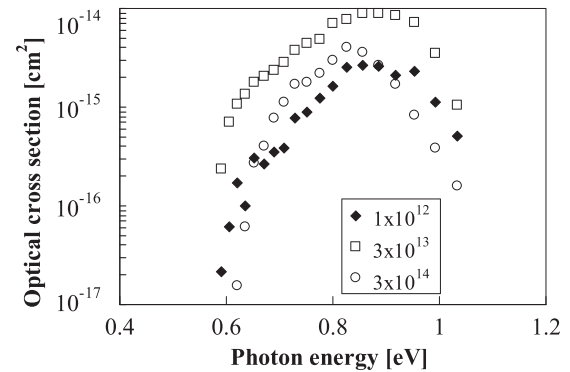


FIG. 4. Optical cross section obtained by the O-CTS measurement as a function of photon energy for the peak 1 defect.

of the order of  $10^{-16}$ – $10^{-15} \text{ cm}^2$ , and there are no significant differences between the samples.  $\sigma_o$  values of the same order of magnitude have been reported for deep impurities in Si.<sup>31</sup>

### III. SIMULATION OF SOLAR CELL PERFORMANCE

#### A. Simulation method

We used AMPS-1D, which is a well-known device simulation tool developed by Fonash *et al.* at the Pennsylvania State University.<sup>32</sup> The structure of the base solar cell is schematically shown in Fig. 5. The top layer is  $n^+$ -Si and there is a back-surface-field (BSF) layer at the bottom. The surface recombination velocity for the minority carriers was assumed to be 100 cm/s. A recombination center was introduced at the mid-gap energy level, and the product of its concentration and capture cross section was set so that the carrier lifetime is 0.1  $\mu\text{s}$  for the top layer, 0.2  $\mu\text{s}$  for the BSF

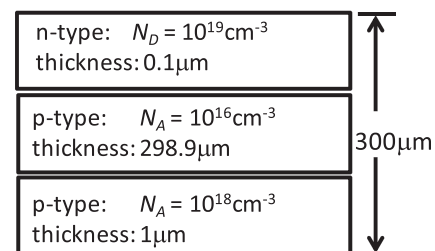


FIG. 5. Structure of the Si solar cell simulated by AMPS-1D.

TABLE II. Concentration and properties of the peak 1 defect.

Dose [cm <sup>-2</sup> ]	N <sub>t</sub> [cm <sup>-3</sup> ]	E <sub>c</sub> - E <sub>t</sub> [eV]	σ <sub>e</sub> [cm <sup>2</sup> ]	σ <sub>h</sub> [cm <sup>2</sup> ]
1 × 10 <sup>12</sup>	1.0 × 10 <sup>14</sup>	0.4	2.3 × 10 <sup>-15</sup>	1.5 × 10 <sup>-15</sup>
3 × 10 <sup>13</sup>	2.0 × 10 <sup>14</sup>	0.4	1.5 × 10 <sup>-14</sup>	1.0 × 10 <sup>-15</sup>
3 × 10 <sup>14</sup>	1.3 × 10 <sup>15</sup>	0.4	2.0 × 10 <sup>-14</sup>	1.5 × 10 <sup>-16</sup>

layer, and 1 μs for the thick p-type layer. For AM1.5 irradiation, the simulated energy conversion efficiency is 17.7%.

Properties of the peak 1 defect are listed in Table II. The defect energy level E<sub>c</sub> - E<sub>t</sub> and capture cross section for electrons σ<sub>e</sub> were obtained from the DLTS data (the Arrhenius plot), neglecting the capture barrier. The capture cross section obtained by the Arrhenius plot is in fact the value at the infinite temperature σ<sub>∞</sub>. If there is a capture barrier (E<sub>cap</sub>), the capture cross section at a temperature T will be σ<sub>∞</sub>exp(-E<sub>cap</sub>/kT), and the activation energy obtained by the Arrhenius plot is also different from the energy level E<sub>c</sub> - E<sub>t</sub> by E<sub>cap</sub>. Here, we assume that E<sub>cap</sub> = 0. The capture cross section for holes σ<sub>h</sub> was estimated as follows: Using AMPS-1D, we first simulated bulk n-type Si having a carrier lifetime value obtained by the lifetime measurement for the unimplanted sample. Then, the peak 1 defect was introduced in the simulation, and its capture cross section for holes was determined so that the calculated carrier lifetime is equal to the observed carrier lifetime. For each implantation dose, we obtained defect parameters separately from the corresponding experimental data. The obtained values of σ are different depending on the dose, as shown in Table II. This will mainly be due to scattering in the data, but may be partly due to the variation in the atomic structure of the defect complexes with the implantation dose.

The absorption coefficient (α) of the sub-band-gap optical absorption due to the peak 1 defect was estimated by the equation

$$\alpha(h\nu) = \sigma_o(h\nu)N_t, \quad (3)$$

where N<sub>t</sub> is the peak 1 defect density. Figure 6 shows α(hν) calculated using σ<sub>o</sub>(hν) given in Fig. 4 and N<sub>t</sub> given in Table II. For comparison, α in the above-band gap range due

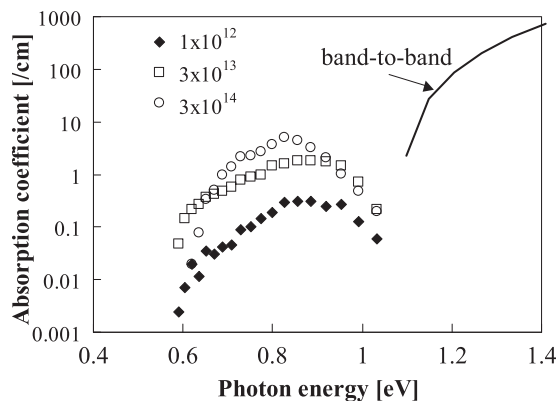


FIG. 6. Absorption coefficient calculated from the optical cross section and concentration of the peak 1 defect. For comparison, the absorption coefficient due to the band-to-band transition is also shown.

to the band-to-band transition is also shown. α due to the defects is of the order of 0.1–1 cm<sup>-1</sup>, which is much smaller than α due to the band-to-band transition. It should be noted that σ<sub>o</sub> obtained by the O-CTS measurement is the cross section for the electron transition from the defect level to the conduction band. Thus, the above equation is based on the assumption that the defects are all occupied by an electron. To generate an electron-hole pair, a valence band electron needs to be excited to the defect level. Unless the cross section for this process is much larger than σ<sub>o</sub> in Fig. 4, the actual absorption coefficient will be smaller than that given by Eq. (3) because the defects are only partially occupied by electrons. Thus, α in Fig. 6 gives the upper limit values, and the actual sub-band-gap absorption should be smaller. As shown below, this does not affect the final result.

## B. Simulation results

Figure 7(a) shows the calculated current-voltage (I-V) curves of the Si solar cell both with and without the implantation-induced defect layer. The defect layer is 1-μm-thick and is placed at the pn junction (in the p-type layer of the junction). The defect density is assumed to be constant (equal to N<sub>t</sub> listed in Table II) within the defect layer. The solar cell parameters deduced from these I-V curves are listed in Table III. As shown in the figure and the table, the open-circuit voltage (V<sub>oc</sub>) decreases with increasing implantation dose (defect density). This is because the defects act as a recombination center for majority carriers, and thus enhance the recombination current (forward dark current). The short-circuit current (I<sub>sc</sub>) decreases slightly with the introduction of the defect layer. As noted in the Introduction, the defect level may increase the photocurrent by acting as a stepping stone for the sub-band-gap absorption, but it simultaneously may also decrease the photocurrent by acting as a recombination center for minority carriers. The calculation

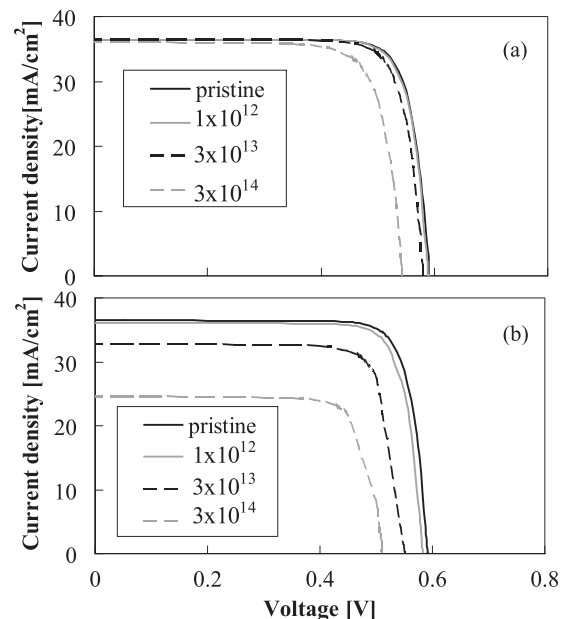


FIG. 7. Calculated I-V characteristics of the solar cell with a defect layer at the pn junction. The defect layer thickness is 1 μm for (a) and 10 μm for (b).

TABLE III. Calculated solar cell parameters of the cells with a 1- $\mu\text{m}$ -thick defect layer. The concentration and properties of the defect are assumed to be related to the dose, as shown in Table II.

Dose [ $\text{cm}^{-2}$ ]	$I_{\text{sc}}$ [ $\text{mAcm}^{-2}$ ]	$V_{\text{oc}}$ [V]	Fill factor	$\eta$ [%]
No	36.46	0.59	0.82	17.69
$1 \times 10^{12}$	36.46	0.59	0.82	17.60
$3 \times 10^{13}$	36.42	0.58	0.81	17.13
$3 \times 10^{14}$	36.06	0.54	0.78	15.29

results show that the enhancement in  $I_{\text{sc}}$  due to the sub-band-gap absorption is negligible because the absorption coefficient due to the defects is very small, as shown in Fig. 6. (As noted above, the actual absorption coefficient is expected to be even smaller than that shown in Fig. 6.) On the other hand, since  $I_{\text{sc}}$  decreased only slightly, the effects of the enhanced recombination for minority carriers are also not significant. This is because electron-hole pairs generated within the defect layer can be separated effectively owing to the depletion region, which extends to about one third of the defect layer. The diffusion length in the defect layer is several  $\mu\text{m}$ , which is larger than the defect layer thickness, and thus the photo-generated carrier can migrate through the defect layer.

Figure 7(b) shows the calculated I-V curves for the cell with a 10- $\mu\text{m}$ -thick defect layer.  $N_t$  is assumed to be constant within the layer and is the same as for Fig. 7(a). The solar cell parameters deduced from these I-V curves are listed in Table IV. In this case, a considerable part of the photo-generated carriers are lost because of enhanced recombination within the 10- $\mu\text{m}$ -thick defect layer. On the other hand, the photo excitation due to the defect level is still negligible, and thus the net effect of the defect introduction is a decrease in  $I_{\text{sc}}$ .

If the 1- $\mu\text{m}$ -thick defect layer is placed within the BSF layer, no significant change appears in the solar cell performance. The defect layer does not affect the forward-bias characteristics, and thus  $V_{\text{oc}}$  remained unchanged. The excited minority carriers can be swept to the p-type layer due to the electric field at the p-type-layer/BSF interface, and thus enhancement of the recombination is not significant. The photo absorption due to the defect level is negligible, and thus no improvement or deterioration was found in the solar cell properties.

### C. Discussion

The simulation shows that the efficiency decreases rather than increases due to defect introduction. This is

TABLE IV. Calculated solar cell parameters of the cells with a 10- $\mu\text{m}$ -thick defect layer. The concentration and properties of the defect are assumed to be related with the dose, as shown in Table II.

Dose [ $\text{cm}^{-2}$ ]	$I_{\text{sc}}$ [ $\text{mAcm}^{-2}$ ]	$V_{\text{oc}}$ [V]	Fill factor	$\eta$ [%]
No	36.46	0.59	0.82	17.69
$1 \times 10^{12}$	36.07	0.58	0.82	17.18
$3 \times 10^{13}$	32.79	0.55	0.81	14.52
$3 \times 10^{14}$	24.68	0.51	0.79	9.92

because the photo absorption via the defect level is so weak that the additional carrier excitation is negligible, and the defect level acts as a recombination center to increase the forward dark current and decrease the photo current. The rate of the sub-band-gap photo absorption is determined by the optical cross section  $\sigma_o$ , and the rate of the recombination by the capture cross section  $\sigma_e$  and  $\sigma_h$ . Therefore, one can expect that the efficiency will increase if  $\sigma_o$  is sufficiently large, or if  $\sigma_e$  and  $\sigma_h$  are sufficiently small. To see how large  $\sigma_o$  needs to be for the realization of an efficiency improvement, we calculated the efficiency assuming  $\sigma_o$  values that were larger than the actual one. Figure 8 shows the variation of the efficiency with  $\sigma_o$ . The defect layer is 1- $\mu\text{m}$ -thick and is placed at the pn junction. For the low dose (small  $N_t$ ), a small improvement in efficiency will be attained when  $\sigma_o > 10^{-12} \text{ cm}^2$ , i.e., is more than three orders of magnitude larger than the actual value. It is not plausible that a deep level defect can have such a large  $\sigma_o$ , since the reported value of  $\sigma_o$  for impurities in Si are all in the range of  $10^{-16}$ – $10^{-15} \text{ cm}^2$ .

The photo absorption via the defect level can be effectively enhanced by optical trapping. If the light is reflected at both of the surfaces, it can travel through the cell repeatedly and have a greater chance of being absorbed. However, the above calculation indicates that for realizing significant efficiency improvement, the light needs to go through the cell more than one thousand times so that the absorption is enhanced by three orders of magnitude. Therefore, it is not realistic to increase the photo current by optical trapping alone.

Another possible way of improving the efficiency is to find a defect with small capture cross sections  $\sigma_e$  and  $\sigma_h$ . As shown in Table II,  $\sigma_e$  and  $\sigma_h$  are of the order of  $10^{-15}$ – $10^{-16} \text{ cm}^2$ . If they are smaller by three orders of magnitude,  $N_t$  can be increased by three orders of magnitude without further deteriorating the I-V characteristics. Then, the absorption will be enhanced by three orders of magnitude and the efficiency can be improved. This can be generalized as follows: If the thermal capture cross section is more than three orders of magnitude smaller than the optical cross section, it may be possible to increase the efficiency. In fact, a capture cross section of less than  $10^{-19} \text{ cm}^2$  is not unusual for defects in

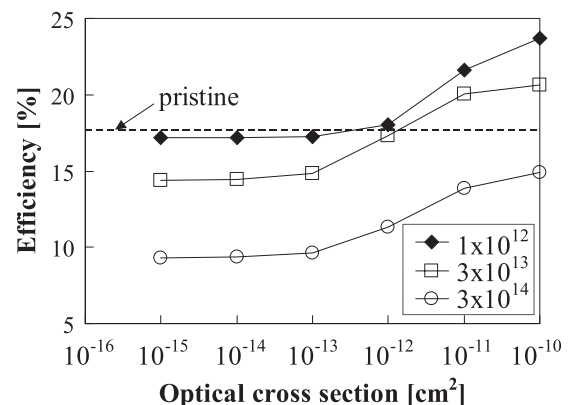


FIG. 8. Calculated efficiencies of the solar cell with a 1- $\mu\text{m}$ -thick defect layer at the pn junction. The optical cross section  $\sigma_o$  is assumed to be a variable, and other properties are fixed, as shown in Table II.

semiconductors. In the carrier lifetime measurement, a slow component sometimes appears in an excess carrier decay curve because of a minority carrier trap, i.e., a defect with a very small capture cross section for majority carriers.<sup>33</sup> Such a trap may, in principle, be used to improve the efficiency of IL solar cells.

#### IV. CONCLUSION

We have characterized the defects introduced by hydrogen implantation into Si. The energy level and the capture cross sections were obtained by DLTS and  $\mu$ -PCD measurements, while the optical cross section was evaluated by O-CTS. Based on the defect properties thus obtained, we simulated the characteristics of a solar cell having a defect layer in it. The results showed that it is not possible to improve the efficiency with defects that have been induced by hydrogen implantation.

Such a basic investigation of carrier capture and optical excitation has to be done for any energy level being considered for IL solar cells. It should again be highlighted that without performing an evaluation of the actual properties of IL (native defects, impurities, quantum dots, etc.), we cannot conclude whether or not the efficiency can be improved by that level.

#### ACKNOWLEDGMENTS

We would like to thank Messrs H. Uno and H. Sakane of S.H.I. Examination & Inspection, Ltd., for performing hydrogen implantation and also for financial support.

<sup>1</sup>W. Shockley and H. Queisser, *J. Appl. Phys.* **32**, 510 (1961).

<sup>2</sup>M. Wolf, *Proc. IRE* **48**, 1246 (1960).

<sup>3</sup>A. Luque and A. Martí, *Phys. Rev. Lett.* **78**, 5014 (1997).

<sup>4</sup>H. Kasai and H. Matsumura, *Sol. Energy Mater. Sol. Cells* **48**, 93 (1997).

<sup>5</sup>P. Würfel, *Sol. Energy Mater. Sol. Cells* **79**, 153 (2003).

<sup>6</sup>M. Y. Levy and C. Honsberg, *Phys. Rev. B* **78**, 165122 (2008).

<sup>7</sup>A. S. Brown and M. A. Green, *J. Appl. Phys.* **94**, 6150 (2003).

<sup>8</sup>K. Yoshida, Y. Okada, and N. Sano, *J. Appl. Phys.* **112**, 084510 (2012).

<sup>9</sup>R. Strandberg and T. W. Reenaas, *Prog. Photovoltaics* **20**, 431 (2012).

<sup>10</sup>A. S. Lin, W. Wang, and J. D. Phillips, *J. Appl. Phys.* **105**, 064512 (2009).

<sup>11</sup>A. Luque, A. Martí, E. Antolín, and C. Tablero, *Physica B* **382**, 320 (2006).

<sup>12</sup>E. Antolín, A. Martí, J. Olea, D. Pastor, G. González-Díaz, I. Martíl, and A. Luque, *Appl. Phys. Lett.* **94**, 042115 (2009).

<sup>13</sup>J. J. Krich, B. I. Halperin, and A. Aspuru-Guzik, *J. Appl. Phys.* **112**, 013707 (2012).

<sup>14</sup>M. J. Keevers and M. A. Green, *J. Appl. Phys.* **75**, 4022 (1994).

<sup>15</sup>M. Schmeits and A. A. Mani, *J. Appl. Phys.* **85**, 2207 (1999).

<sup>16</sup>S. Zh. Karazhanov, *J. Appl. Phys.* **89**, 4030 (2001).

<sup>17</sup>J. Yuan, H. Shen, H. Huang, and X. Deng, *J. Appl. Phys.* **110**, 104508 (2011).

<sup>18</sup>J. Li, M. Chong, J. Zhu, Y. Li, J. Xu, P. Wang, Z. Shang, Z. Yang, R. Zhu, and X. Cao, *Appl. Phys. Lett.* **60**, 2240 (1992).

<sup>19</sup>C. Summonte, M. Biavati, E. Gabilli, R. Galloni, and S. Guerri, *Appl. Phys. Lett.* **63**, 785 (1993).

<sup>20</sup>K. W. J. Barnham and G. Duggan, *J. Appl. Phys.* **67**, 3490 (1990).

<sup>21</sup>N. G. Anderson, *Physica E* **14**, 126 (2002).

<sup>22</sup>V. Popescu, G. Bester, M. C. Hanna, A. G. Norman, and A. Zunger, *Phys. Rev. B* **78**, 205321 (2008).

<sup>23</sup>V. P. Kunets, C. S. Furrow, T. Al. Morgan, Y. Hirono, M. E. Ware, V. G. Dorogan, Yu. I. Mazur, V. P. Kunets, and G. J. Salamo, *Appl. Phys. Lett.* **101**, 041106 (2012).

<sup>24</sup>S. M. Hubbard, C. D. Cress, C. G. Bailey, R. P. Raffaele, S. G. Bailey, and D. M. Wilt, *Appl. Phys. Lett.* **92**, 123512 (2008).

<sup>25</sup>D. Guimard, R. Morihara, D. Bordel, K. Tanabe, Y. Wakayama, M. Nishioka, and Y. Arakawa, *Appl. Phys. Lett.* **96**, 203507 (2010).

<sup>26</sup>Y. Okada, R. Oshima, and A. Takata, *J. Appl. Phys.* **106**, 024306 (2009).

<sup>27</sup>Y. Nakakura, M. Kato, M. Ichimura, E. Arai, Y. Tokuda, and S. Nishino, *J. Appl. Phys.* **94**, 3233 (2003).

<sup>28</sup>M. Kato, S. Tanaka, M. Ichimura, E. Arai, S. Nakamura, T. Kimoto, and R. Pässler, *J. Appl. Phys.* **100**, 053708 (2006).

<sup>29</sup>L. Palmetshofer and J. Reisinger, *J. Appl. Phys.* **72**, 2167 (1992).

<sup>30</sup>Y. Tokuda, H. Shimada, and A. Ito, *J. Appl. Phys.* **86**, 5630 (1999).

<sup>31</sup>M. Okuyama, N. Matsunaga, J.-W. Chen, and A. G. Milnes, *J. Electron. Mater.* **8**, 501 (1979).

<sup>32</sup>See <http://ampsmodeling.org/>, where one can download software AMPS (Analysis of Microelectronic and Photonic Structures), developed by the group of Prof. S. Fonash.

<sup>33</sup>J. W. Orton and P. Blood, *The Electrical Characterization of Semiconductors* (Academic Press, London, 1990).